Removal of iron, aluminium, manganese and copper from leach solutions of lithium-ion battery waste using ion exchange

Virolainen Sami, Wesselborg Tobias, Kaukinen Arttu, Sainio Tuomo

DOI: 10.1016/j.hydromet.2021.105602

Hydrometallurgy 202 (2021) 105602

Contents lists available at ScienceDirect

Hydrometallurgy

journal homepage: www.elsevier.com/locate/hydromet

Removal of iron, aluminium, manganese and copper from leach solutions of lithium-ion battery waste using ion exchange

Sami Virolainen *, Tobias Wesselborg, Arttu Kaukinen, Tuomo Sainio

LUT University, School of Engineering Science, Department of Separation Science, Yliopistonkatu 34, FI−53850 Lappeenranta, Finland

ARTICLE INFO

Keywords:
Lithium ion battery
Recycling
Ion exchange
Aminomethylphosphonic acid

ABSTRACT

The shift to electric mobility necessitates recycling the metals from lithium ion battery waste. Ion exchange was studied for use in the removal of impurities from synthetic lithium ion battery waste leachate in laboratory-scale batch and column experiments. Aminomethylphosphonic acid functional chelating resin (Lewatit TP260) was capable of removing Fe, Al, Mn, and Cu from the leachate, while leaving valuable Co, Ni, and Li as a pure mixture in the raffinate. Increasing the pH up to 3 and the temperature to 60 °C improved the purity and productivity. Iron and aluminium could not be eluted efficiently by mineral acids, but an oxalate solution was found feasible. A two-step elution procedure, in which Cu and Mn are first removed with sulfuric acid, followed by Fe and Al removal with potassium oxalate, was successfully demonstrated. The suggested process produced a > 99.6% pure Li + Co + Ni solution (battery grade), along with a Mn and Cu rich sulfuric acid solution with Co as an impurity and an oxalate solution of Fe + Al as by-products. The productivities for these solutions were 0.39, 0.16, and 0.38 BV/h, respectively. The Co loss was very low (1.1%) as compared to previously suggested impurity removal processes using precipitation and solvent extraction. Moreover, Co can be easily recycled back to the ion exchange column feed after Mn and Cu are recovered as pure by-products.

1. Introduction

Currently, the world is quickly moving toward electric mobility, and lithium ion batteries (LIBs) have a key role to play in this societal change because they are, at least in short- to medium-term, the only reasonable energy storage units. The use of LIBs in other electronic devices has also been growing, leading to rapidly increasing demand for the associated raw material metals needed. For example, the one million electric vehicles sold in 2017 contain 250 kt (500,000 m^3) of battery material (Harper et al., 2019) and in 2025 the collected LIB waste amount from EVs is estimated to be 600 kt Recycling only this amount would require at least a five-fold increase as compared to the current worldwide recycling capacity (Ferg et al., 2019). Depending on the cathode material, an entire LIB contains 47–79% (w/w) metals (Winslow et al., 2018).

The estimated lifespan of LIBs is 3–10 years (Xiao et al., 2020), meaning that recycling them is an important issue from many points of view. Firstly, they contain hazardous materials, such as metals (Li, Co, Ni, Mn, Fe, and Al) and electrolytes ($LiPF_6$, $LiBF_4$, ethylene carbonate, and dimethyl carbonate), which must be removed in order to avoid negative environmental and health impacts(Meshram et al., 2020; Younesi et al., 2015; Harper et al., 2019). Secondly, they represent a potentially sustainable valuable metals source.

The composition of LIB waste varies a great deal depending on the type of waste batteries and the pre-treatment process used (pyrometallurgical and/or mechanical). The metal content is typically Co 5–30%, Ni 0–10%, Li 2–12%, Al 3–10%, Fe 0–25%, Mn 5–12%, and Cu 7–17% (Zeng et al., 2014; Porvali et al., 2019). Generally, of these metals, Co, Ni, and Li are usually seen as valuable and having recovery interest. The remainder are impurities.

Lithium-ion battery recycling begins with discharging and dismantling (only EV batteries). Then, the LIB waste undergoes mechanical pretreatment. After this, the recycling can be accomplished via either the hydro- or pyrometallurgical route or a combination of these (Georgi-Maschler et al., 2012; Ekberg and Petranikova, 2015; Li et al., 2018; Quintero-Almanza et al., 2019; Xiao et al., 2020).

The hydrometallurgical LIB waste recycling process begins with acid leaching. The most popular lixiviant is H_2SO_4, and some reductant, usually H_2O_2, is needed to reduce the Co and Mn to a divalent state (Harper et al., 2019). The metal composition of LIB waste leachate (later LIBWL) obtained by H_2SO_4/H_2O_2 leaching is Fe 0.5–3.6, Al 0.6–2.4, Cu

* Corresponding author.
E-mail address: Sami.Virolainen@lut.fi (S. Virolainen).

https://doi.org/10.1016/j.hydromet.2021.105602
Received 27 September 2020; Received in revised form 29 March 2021; Accepted 3 April 2021
Available online 20 April 2021

1.8–2.6, Mn 1.8–9.6, Co 6.5–44.7, Ni 0.5–9.7, and Li 1.0–5.4 g/L (Dorella and Mansur, 2007; Swain et al., 2007; Ferreira et al., 2009; Chen et al., 2011; Chen et al., 2015a; Chen et al., 2015b; Sattar et al., 2019; Peng et al., 2020). The acidity (or pH) of the leachates is seldom mentioned, but evidently, the acidity is high, with reported pH values of 0.17–0.70 (Mendes and Martins, 2005; Kang et al., 2010; Peng et al., 2020).

After leaching, the most common methods used to separate, purify, and recover the metals are precipitation and solvent extraction (Meshram et al., 2020). Also, impurities (Fe, Al, Mn, and Cu) have been removed via precipitation and/or solvent extraction. However, in these processes, especially precipitation, there are problems with selectivity; i.e., if the impurities are removed with a high yield, there are also significant losses of valuable metals. Selectivity between Mn and Co is especially low, and it will represent significant drawback to the techno-economical efficiency of this process if significant amounts of the most valuable metal, Co, are lost in the purification step (Peng et al., 2020; Xiao et al., 2020).

To our knowledge, there is only one scientific paper about the utilization of ion exchange in recycling metals from LIB waste. Chiu and Chen (2017) successfully tested, in batch experiments, several chelating resins (iminodiacetic acid, bispicolylamine, and phosphinic acid) for the sorption of Ni and Co from Mn-containing LIBWL, but selectivity is not discussed in the paper. In addition, there are three patents describing ion exchange in LIB recycling (Harris and White, 2018; Chai et al., 2019a, 2019b); however, ion exchange does not play a major role in impurity removal in these patents.

Even though ion exchange has not yet been utilized in hydrometallurgical LIB recycling, it can likely offer the high selectivities needed in the fractionation of the complex mixture. In this research, the ion exchange purification of LIBWL is discussed for the first time. According to the literature (Table 1) Fe, Al, and Cu should be easily removed, but there are no references indicating selectivity for Mn over Co and Ni. The goal here is to remove all the impurities (Fe, Al, Mn, and Cu) to produce a battery-grade pure (>99.5%) Li + Co + Ni mixture, construct an initial flowsheet proposal, and provide proof of concept for such. First, a suitable commercial ion exchange resin and process parameters (feed-pH and T) for the loading step are chosen based on column breakthrough experiments. Then, an efficient elution scheme for a chelating resin is designed, and finally, several loading-elution cycles are executed to demonstrate the repeatability of the suggested sequence and study-related process-technical details.

2. Materials and methods

2.1. Materials

The chemicals used in experiments are presented in Table 2.

Table 1
Selectivity orders of commercially available ion exchange resins for LIB metals.

Functional group	Commercial example(s)	Selectivity order	Reference(s)
Bispicolylamine	Dowex M4195	Cu > Ni > Fe (III) > Co	(Chiu and Chen, 2017; Flett, 2004)
Iminodiacetic acid	Amberlite IRC 748 Purolite S930 Lewatit TP207	Fe(III) > Cu > Ni > Co > Fe(II) > Mn	(Zainol and Nicol, 2009; Siqueira et al., 2011; Jurrius et al., 2014; Chiu and Chen, 2017)
Aminophosphonic acid	Purolite S950	Fe(III) > Cu > Al(III) > Ni > Co(II)	(Fisher and Treadgold, 2008)
Aminomethylphosphonic acid	Lewatit TP260	Fe(III) > Cu > Ni > Co(II)	(LANXESS, 2011; Sainio and Suppula, 2015)

Table 2
Chemicals used in the ion exchange experiments for purifying LIBWL.

Chemical	Supplier	Purity, %
$Al_2(SO_4)_3{\cdot}18H_2O$	PROLABO	>95
$CoSO_4{\cdot}7H_2O$	Alfa Aesar	98
$CuSO_4$	VWR Chemicals	99
$Fe_2(SO_4)_3{\cdot}xH_2O$	Alfa Aesar	>95
$Li_2SO_4{\cdot}H_2O$	Alfa Aesar	99
$MnSO_4{\cdot}H_2O$	Alfa Aesar	99
$NiSO_4{\cdot}6H_2O$	Sigma-Aldrich	99
H_2SO_4	Merck	95–97
NaOH	Merck	>99

Four commercial ion exchange resins, one strong and one weak cation exchanger and two chelating resins, were used in the experiments. Their properties are summarised in Table 3. The bed porosities (void fractions) of the resin beds were measured by injecting Blue Dextran pulses into the packed resin beds. Resins were pretreated with NaOH-H_2O-HCl cycles, ultimately leaving the resins in acid form. The resin bed volumes were measured in H_2O.

A synthetic leachate based on metal concentrations given in Porvali et al. (2019) was used as a feed solution. The one alteration was that, here, the solution was made in sulfate media (1 M H_2SO_4) instead of chloride media, as in the reference. The analyzed composition and properties of the feed solution are presented in Table 4. The Redox-potential E varied between 521 and 538 mV and describes the regular analysis performed during the project. The metals' concentrations are averages of 18 ICP-MS determinations.

2.2. Column experiments

Jacketed glass columns of 15 mm-diameter purchased from YMC Europe GMBH were used in the experiments. The synthetic leach liquor was fed to the column from the bottom. Experiments for the comparison of the resins consisted of a loading-H_2O wash-2.0 M H_2SO_4 elution-H_2O wash cycle. In the loading and elution steps, the flowrate was 2.0 BV/h, the sampling interval was 2 min, and their durations were 6.0 and 3.5 BV, respectively. The H_2O washes were run from top to bottom at 6.0 BV/h for 2.0 BV.

Two multicycle runs were performed to study the elution of the resins and have them be regenerated so that there will be constant impurity removal capacity over several cycles. In the first multicycle experiment (four cycles), 2.0 M H_2SO_4 was used as an eluent and the temperatures in the feed and elution steps were 60 and 25 °C, respectively. In the second multicycle experiment (three cycles), both 2.0 M H_2SO_4 and 0.4 M potassium oxalate solutions were used as eluents (flowrate 2.0 BV/h, except H_2O washes 6.0 BV/h, T = 60 °C), but adjustments to the elution step configuration were made based on observations after each cycle. These adjustments are discussed with the results.

2.3. Sorption equilibrium experiments

To verify the LIBWL metals' sorption behavior, in the breakthrough experiments, to the Lewatit TP260 resin, a series of batch experiments was performed by shaking 2 g water swollen resin and 8 mL of the LIBWL solution (accurate amounts weighed) with varying pH levels in test tubes overnight at room temperature (22–23 °C). The LIBWL samples were analyzed before and after the shaking, and the extent of sorption, as a function of equilibrium pH, was determined based on the masses of metals, Me:

$$E = \frac{m^0_{Me} - m^{eq}_{Me}}{m^0_{Me}} \cdot 100\% \quad (1)$$

The masses were used because the volume of the LIBWL was larger after equilibration due to the shirking of the water-swollen resin and the

Table 3
Ion exchange resins used in the ion exchange experiments to purify LIBWL.

	Lewatit TP260	Purolite S-930	Finex CS12GC	Finex CA16GC
Type	Chelating	Chelating	Strong cation	Weak cation
Functional group	Aminomethylphosphonic acid	Iminodiacetic acid	Sulfonic acid	Carboxylic acid
Bed porosity	0.423	0.430	–	–

Table 4
Composition and properties of the synthetic LIB leachate solution used in the ion exchange experiments.

Element	Al	Fe	Mn	Cu	Co	Ni	Li
Concentrations in g/L	1.30 ± 0.14	0.64 ± 0.30	2.03 ± 0.21	1.66 ± 0.18	13.2 ± 1.29	1.60 ± 0.16	3.87 ± 0.48

fact that some amount of the metals migrated to the resin pores without selective sorption.

2.4. Batch elution experiments

Batch elution experiments were performed for the Lewatit TP260 resin loaded in batch with synthetic LIBWL at a pH of 1.8 and L/S = 150 mL:7 g at room temperature (22–23 °C) for 24 h. Seven eluents were studied in varying concentrations (Table 5). Samples (L/S = 40 mL:2 g) were shaken for 64 h at room temperature. The eluents were compared based on aqueous phase ICP-MS analyses of the eluent samples.

2.5. Analytical methods

Metal concentrations from liquid-phase samples were analyzed with ICP-MS (Agilent 7900). Solid phase (resin) metal concentrations were measured by first digesting the samples with Milestone Ultrawave microwave digestion system in reversed aqua regia (3,1 mixture of concentrated HNO_3 and HCl). Samples for the ICP-MS analyses were diluted with a 1:1 (% *v*/v) mixture of concentrated HNO_3 and HCl. Redox potential measurements were performed with a Mettler Toledo FiveGo handheld device with an LE510 Ag/AgCl electrode.

3. Results and discussion

3.1. Choice of the resin and effects of feed-pH, temperature, and column height

The strong (Finex GS12GC) and weak (Finex GA16GC) cation exchangers were not capable of removing the impurity metals selectively from the LIBWL, and iminodiacetic acid functional chelating resin (Purolite S930) selectively removed only Fe and Cu. As expected based on the previous literature (Table 1), aminomethylphosphonic acid functional chelating resin (Lewatit TP260) selectively removed Fe, Cu, and Al. Now, the new breakthrough results reveal that Mn can also be removed (Fig. 1). This is a remarkable result because, in hydrometallurgical LIBWL separation processes, all four impurity metals have not been separated in a single-unit process before. In precipitation, the selectivities over Co are too low (Wang and Friedrich, 2015; Peng et al., 2020), and in solvent extraction, the problem is that the co-extraction of Co is significant under conditions in which Cu and Mn are extracted (Cheng, 2000). The Lewatit TP260 resin was chosen as the only separation material for further studies.

Table 5
Eluents and their concentrations in studying the elution of LIBWL-loaded Lewatit TP260 resin.

Eluent	Concentrations, mol/L
H_2SO_4	1, 2, 4, 6
HNO_3	1, 2, 4, 6
HCl	1, 2, 4, 6
HCl (1 mol/L) + NaCl	Saturated, 2, 1, 0.5
Sodium citrate ($Na_3C_6H_5O_7$)	1.6, 0.8, 0.4, 0.2
Potassium oxalate ($K_2C_2O_4$)	0.5, 0.4, 0.3, 0.2
Tetrasodium EDTA ($C_{10}H_{12}N_2Na_4O_8$)	1.0, 0.5, 0.25, 0.125

Because the goal of the LIBWL purification process is to obtain the purest possible raffinate of Co, Ni and Li, the single-metal breakthrough profiles do not provide the most essential information. Rather, the cumulative purity (*Pu*) does. It is expressed as the mass ratio of Co, Ni and Li as compared to all LIBWL metals, defined as follows:

$$Pu = \frac{\sum(m_{Co} + m_{Ni} + m_{Li})}{\sum(m_{Co} + m_{Ni} + m_{Li} + m_{Cu} + m_{Mn} + m_{Fe} + m_{Al})} \quad (2)$$

in which m_i is the cumulative mass collected for each metal.

Increasing temperature improved the purification performance significantly, and at 60 °C larger volume of solution of Co, Ni and Li with battery-grade purity was collected compared to that collected at 25 °C (Fig. 2). At 60 °C, all the impurity metals were removed more efficiently, but as compared to 25 °C, the removal of Al and Cu was significantly affected compared to that of Mn (Fig. 3a and b).

Using a feed solution without pH adjustment (1 M H_2SO_4), Cu, Mn, and Al broke through immediately at void volume (data not shown), and therefore, it was evident that the pH must be increased significantly to improve the sorption efficiency. This behavior was verified by the pH-dependency equilibrium data (Fig. 4) because the sorption of especially Cu and Mn was significantly improved when the equilibrium-pH was increased from 0.1 to 1.8. When the pH was increased above 1.8, Fe began precipitating, and therefore, this was chosen as the feed pH for the following experiments. A feed pH of 3.0 was also tested after first filtering the precipitated Fe from the solution. The Fe concentration after the filtration was 37 mg/L. The highest purities were obtained at 60 °C and with a feed pH of 3.0 (Fig. 2), and removal of Cu was much more efficient at higher pH values (Figs. 3b and c). A note should be made that the c/c^0 values exceeding unity represent the fact that the already sorbed to the resin metals are replaced by the more affinity having ones. The significantly improved selectivity of the Lewatit TP260 for Cu over the other LIBWL metals was also observed in the batch equilibrium data (Fig. 4). However, it should be noted that the difference in purification performance at a feed pH of 3.0 as compared to 1.8 was not that significant, especially considering that most of the Fe was already removed due to the pH adjustment.

One remarkable observation was that, when a longer bed with same diameter and flowrate in BV/h was used, the overall purification performance was worse than with the shorter bed (Fig. 2). In general, making the bed longer should improve the sorption because the number of mass transfer units is increased. However, in this case, the mass transfer of Al was improved so greatly that Mn and Cu were displaced (Fig. 3c and d), making the overall performance worse. Thus, conditions of feed-pH = 1.8, T = 60 °C, and h_{bed} = 0.150 m were chosen for further process studies.

3.2. Choice of eluents

In the breakthrough experiments discussed in Section 3.1, elution was always performed with 2.0 M H_2SO_4. In principle, the elution curves look normal and reach $c/c^0 < 0.011$ at 3.1 BV, with exception of Al

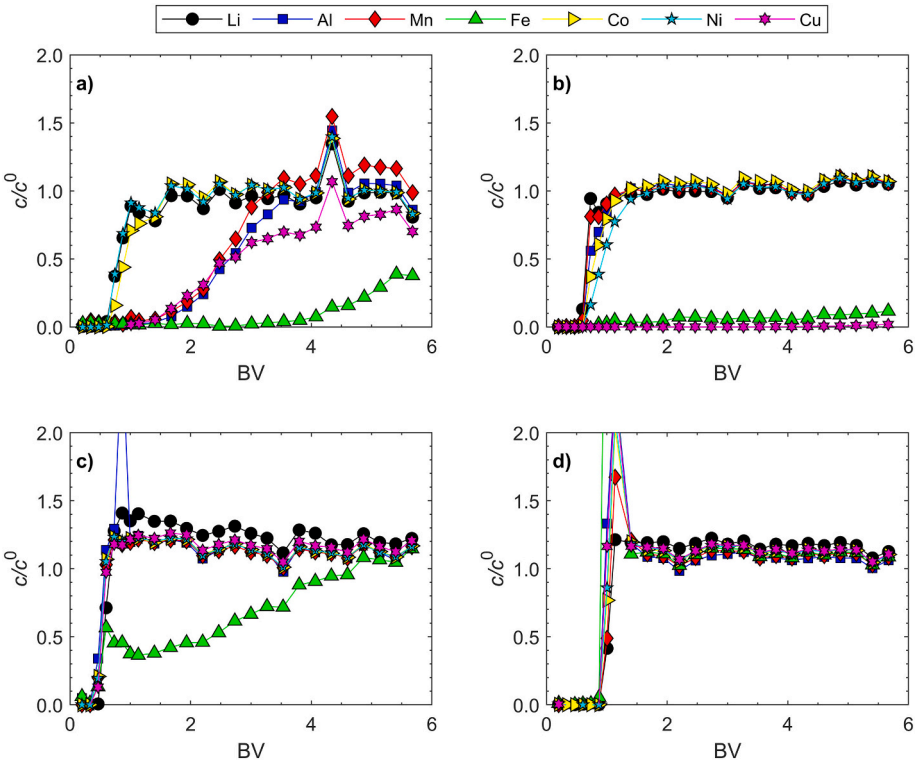

Fig. 1. Breakthrough curves for LIBWL metals with the four studied resins (Table 2). $T = 25$ °C, feed-pH = 1.8, $V_{bed} = 26.7–29.0$ mL, Flowrate = 2.0 BV/h. a) Lewatit TP260 (aminomethylphosphonic acid functionality), b) Purolite S-930 (iminodiacetic acid), c) Finex CA16GC (carboxylic acid), and d) Finex CS12GC (sulfonic acid).

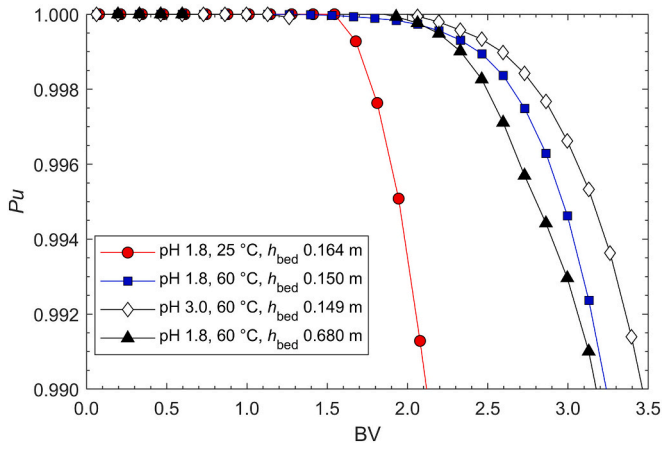

Fig. 2. Cumulative purity curves for Li, Co and Ni (Eq. 2) in LIBWL during impurity removal with aminomethylphosphonic acid functional Lewatit TP260 resin. Flowrate = 2.0 BV/h.

tailing at 0.13 (Fig. 5). However, it was observed in analysis of the resin beds that there were significant amounts of Fe and Al remaining (7.1 and 4.5 mg/g resin, respectively), while other metals were eluted quantitatively (<0.02 mg/g). This leads to deteriorated purification performance, which was observed when running the loading-elution (H_2SO_4) cycles four times consequently. Several references describe the difficulty of eluting Fe(III) from chelating resins, especially aminomethylphosphonic acid type (Sole et al., 2016; Zhang et al., 2016; Virolainen et al., 2019), and some reducing and/or chelating agents (oxalate, H_2SO_3 and Cu(I)) must be used. Lv et al. (2019) also studied Al (III) elution from mixed sulfonic and monophosphonic acid functional resin and observed that, with mineral acids, very high acidities (>4 M) are needed for efficient removal.

To find a suitable eluent for Fe and Al, seven chemicals (Table 5) were tested in batch experiments. The performance of eluents were compared with that of 2.0 M H_2SO_4 by defining normalized elution efficiency:

$$\text{Normalized efficiency} = \frac{c_i^{\mathrm{E}}}{c_i^{\mathrm{H_2SO_4}}} \tag{3}$$

where c_i^{E} is the concentration of metal i in eluent E. For Al elution, potassium oxalate clearly provided the best elution efficiency, being more than six times more efficient than 2.0 M H_2SO_4 (Fig. 6). Increasing the eluent concentration from 0.2 to 0.5 M did not improve the efficiency significantly. Other efficient Al eluents included 6 M HNO_3 and 1.6 M sodium citrate. For Fe, all the eluents with organic ligands showed high elution efficiency. Two eluents, EDTA and oxalate were superior, with >32 normalized efficiency over the entire studied concentration range. Potassium oxalate was slightly better than EDTA, and increasing the potassium oxalate concentration to 0.5 M increased the normalized elution efficiency to 54. Among the mineral acids, 1.0–2.0 M HNO_3 and 6 M HCl showed higher elution efficiency than the 2.0 M H_2SO_4.

The power of potassium oxalate, as a strong eluting agent for Al and Fe, is explained by the very strong chelate-type complexes formed with Fe(III) and Al(III). Oxalate anion has also mild reducing properties ($C_2O_4^{2-} \rightleftarrows CO_2 + 2e^-$, $E^0 = 0.49$ V), being capable of reducing Fe(III) to Fe(II) (Christodoulou et al., 2013; Verma et al., 2019). Because oxalic acid is a diprotic acid, with pK_a values of 1.23 and 4.19 at room temperature, decreasing acidity positively affects its solubility in water and, consequently, complex formation with Al and Fe (Verma et al., 2019). Therefore, here, it was dissolved in KOH having double the concentration of the oxalic acid.

Because Cu and Mn are sparingly soluble ($<2{\cdot}10^{-3}$ mol/L and $<1{\cdot}10^{-3}$ mol/L, respectively) in oxalate media (Soare et al., 2006; Perry et al., 1997), the elution cannot be performed in a single step. Rather, two eluents are needed. The suggested elution scheme is to first elute Cu, Mn, and co-sorbed Co (and traces of Ni) with 2.0 M H_2SO_4 and then elute

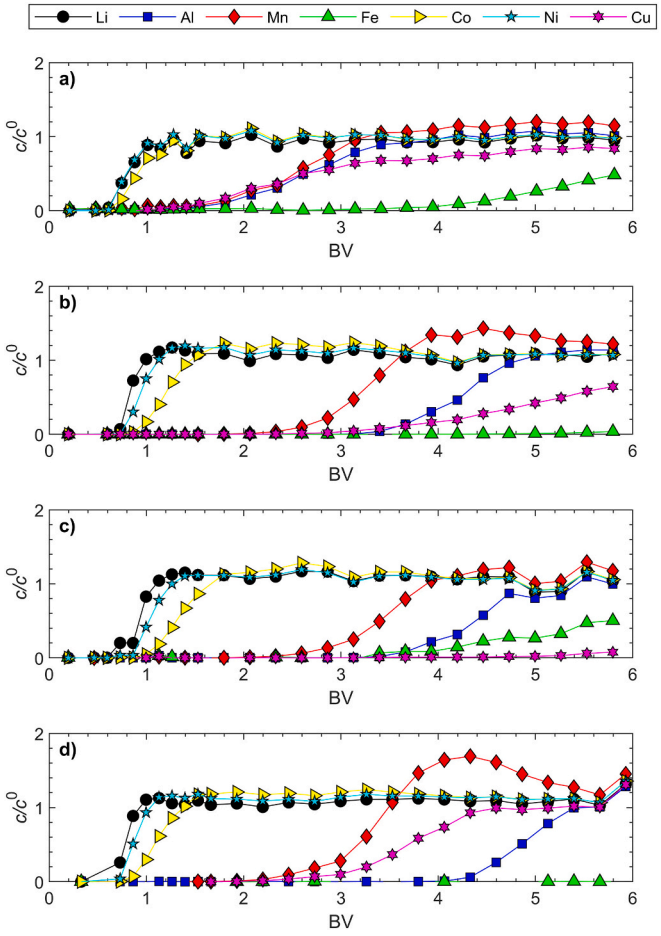

Fig. 3. Breakthrough curves for LIBWL metals with aminomethylphosphonic acid functional Lewatit TP260 resin at various feed pHs, temperatures, and column heights. Flowrate = 2.0 BV/h. a) feed-pH = 1.8, T = 25 °C, h_{bed} = 0.164 m; b) feed-pH = 1.8, T = 60 °C, h_{bed} = 0.150 m; c) feed-pH = 3.0, T = 60 °C, h_{bed} = 0.149 m; d) feed-pH = 1.8, T = 60 °C, h_{bed} = 0.680 m.

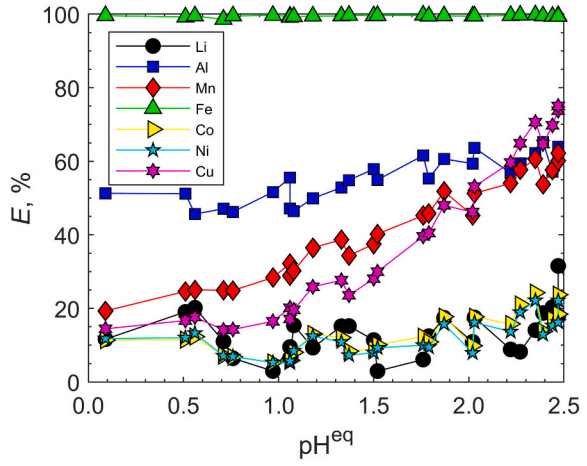

Fig. 4. Sorption equilibrium of LIBWL metals to aminomethylphosphonic acid functional Lewatit TP260 resin at room temperature (22–23 °C).

Fe and Al with 0.4 M potassium oxalate. Fig. 7 presents elution curves for this kind of two-step elution. It can be seen that Cu and Mn are eluted quantitatively, with a slightly tailing profile, by 2.4 BV, with 2.0 M H_2SO_4. The co-sorbed Co and Ni are quantitatively eluted by 1.2 BV. The fraction until this 1.2 BV can be recycled directly back to the feed of the

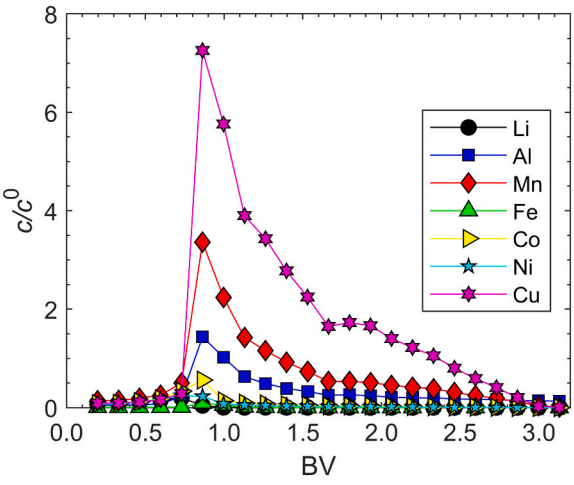

Fig. 5. Elution of the LIBWL metals from aminomethylphosphonic acid functional resin (Lewatit TP260) with 2.0 M H_2SO_4 after loading at a feed pH of 1.8. Flowrate = 2.0 BV/h, T = 60 °C.

loading step. The fraction between 1.2 and 2.4 BV would be a pure mixture of manganese and copper, from which pure Cu and Mn could be obtained as by-products, for example, via the selective solvent extraction of Cu with hydroxyoxime reagent and the consequent precipitation of Mn with carbonate or oxidative precipitation with $KMnO_4$ (Nayl et al., 2015; Meshram et al., 2015; Peng et al., 2020). If the Co-containing fraction is not taken separately by the first 1.2 BV, Co can be recycled back to the loading step feed after removal of Mn and Cu. Aluminium was eluted by 0.4 M potassium oxalate which produced a broad symmetric peak quantitatively, by 2.6 BV, and Fe, with a fronting peak, by 3.2 BV, from the start of the potassium oxalate feed.

In addition to the chemical feasibility of the above two-step elution approach, there are some important details to be considered in terms of configuring the elution cycle. To study these issues, a three-cycle loading-elution run was performed, with appropriate water washes in between the steps (Table 6, Fig. 8). Initially, the resin should be left in H^+ form before the loading step of the next cycle to prevent the carrying over of K into the raffinate product containing Li, Co and Ni. However, as discussed above, Cu has very low solubility in oxalate solution, and if it is fed as the first eluent, precipitation occurs. Precipitation was observed immediately in the three-cycle run when the Cu began eluting, causing delays in and broadening of the Fe elution profile (Fig. 8a). This leads to the conclusion that the H_2SO_4 elution step should be done first but that there should also be a short concentrated H_2SO_4 pulse after the potassium oxalate step to leave the resin in the desired H^+ form.

Secondly, the feed directions (bottom-to-top or top-to-bottom) matter because there are differences in the densities of the eluents: 2 M H_2SO_4 at 60 °C = 1.10 kg/L (Perry et al., 1997) as compared to 0.4 M potassium oxalate at 45 °C = 1.04 kg/L (Behal and Kumar, 2017). The evidence of this is the elution profile of the second cycle (Fig. 8b), when the lighter potassium oxalate was fed from bottom to top, causing the broadening of the elution profiles and incomplete elution due to channeling. When the lighter potassium oxalate was fed from top to bottom, in the third cycle, the elution profiles in both steps became regular like they were in the single-cycle experiment (Fig. 7), and the metals were eluted completely.

3.3. Discussion of the entire suggested ion exchange process

Fig. 9 shows an initial design of the ion exchange process for the purification of LIBWL. The volumes of the produced solutions and their concentrations have been calculated based on the elution curves shown in Fig. 8. According to the loading breakthrough curves measured in this research, the loading must be stopped at 2.8 BV to yield over 99.5% pure

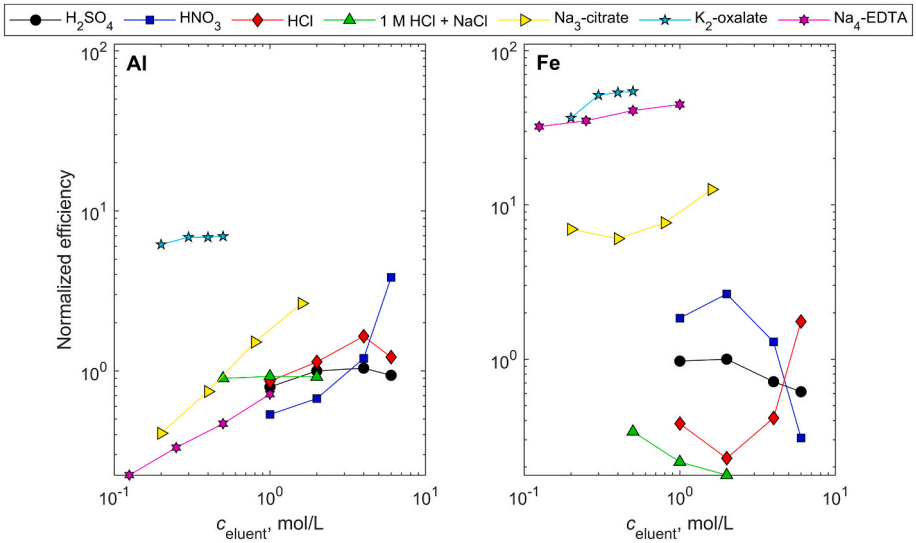

Fig. 6. Batch experiments to determine suitable elution agent and concentration for the removal of Fe and Al from aminomethylphosphonic acid functional resin (Lewatit TP260). L/S = 40 mL/2 g, T = 22–23 °C. Normalized elution efficiency: 2.0 M H_2SO_4 = 1.

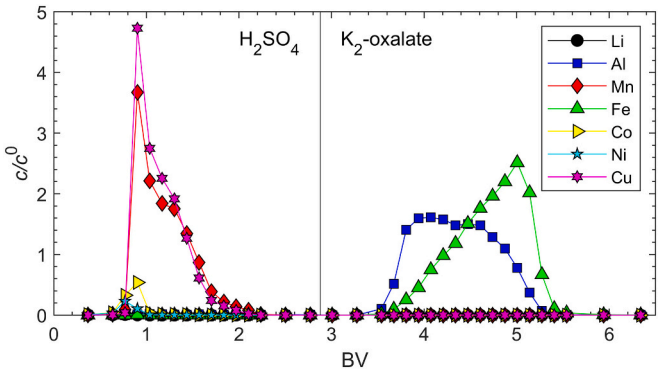

Fig. 7. Two-step elution of the LIBWL metals from aminomethylphosphonic acid functional resin (Lewatit TP260) with 2.0 M H_2SO_4 and 0.4 M potassium oxalate. Resin was loaded at a feed pH of 1.8 for 2.8 BV. The flowrate in all steps was 2.0 BV/h, T = 60 °C.

raffinate containing Li, Co, and Ni. It takes 0.8 BV before the first metal (Li) breaks through, and solution collected until this point is almost pure water, which can be circulated to the water wash feed tanks.

In the suggested process scheme (Fig. 9), after the loading step, the bed is washed with 2.0 BV of water to remove the LIBWL solution from the void fraction of the bed. The composition of the resulting solution is like the original LIBWL but has slightly less of the impurities and is diluted with water. The purpose of this research was not to optimize the length of this step. Rather, excess water was used. It has been shown, in similar ion exchange process design research, that slightly more than one bed volume is sufficient for the physical removal of the metal solution in the void fraction (Virolainen et al., 2019). In a more detailed process design, the length of this step and flowrate used should be optimized to minimize the time and water used.

In the beginning of the first elution step with 2 M H_2SO_4,~ 0.6 BV is pure water, which can be circulated to the water wash feed tank (Figs. 8 and 9). After that, the suggestion is to collect all the metal ions into single fraction to have a Mn- and Cu-rich solution, with mainly Co as an impurity. From the mass balance calculations based on the breakthrough samples' liquid phase analysis, the Co loss from the feed to this eluate is 1.1%, which is significantly less than in the solvent extraction and precipitation processes for impurity removal suggested in the literature (Peng et al., 2020). After the metals have been eluted, there is a small H_2SO_4 fraction free of metal ions, which can be circulated back to the H_2SO_4 feed tank. In the scheme shown in Fig. 9, the length of the H_2SO_4 elution step is 2.5 BV, as in the multicycle experiment (Fig. 8), but it is possible to optimize this down to ca. 1.7 BV. As discussed in Section 3.2, from the eluent fraction obtained in this step, it is possible to produce pure Cu and Mn by-products with known unit operations. After the recovery of Cu and Mn, the Co in raffinate can be recycled back to the ion exchange feed.

In the second elution step, 1.9 BV of pure Al and Fe containing oxalate solution is collected. The collected solution is alkaline because KOH is added to increase the solubility of oxalic acid. According to the solubility calculations (Fig. 10), it is possible to precipitate Al and Fe from the solution by decreasing the pH to 9–10. Oxalate itself is not precipitated, and the raffinate solution may be circulated after increasing the pH with KOH again. One unsolved issue that is a matter to consider for further process design is the question of dealing with the accumulation of potassium salt (depends on the mineral acid used for

Table 6
Three consecutive loading-elution cycle runs for removal of impurity metals from LIBWL with aminomethylphosphonic acid resin (Lewatit TP260).

Cycle 1			Cycle 2			Cycle 3		
Step	Flow direction	BV	Step	Flow direction	BV	Step	Flow direction	BV
Loading	Bottom-to-top	2.78	Loading	Bottom-to-top	2.78	Loading	Bottom-to-top	2.78
H_2O wash	Top-to-bottom	2.00	H_2O wash	Top-to-bottom	2.00	H_2O wash	Top-to-bottom	2.00
$K_2C_2O_4$ elution	Bottom-to-top	2.78	H_2SO_4 elution	Bottom-to-top	2.51	H_2SO_4 elution	Bottom-to-top	2.51
H_2SO_4 elution	Bottom-to-top	2.67	$K_2C_2O_4$elution	Bottom-to-top	2.67	$K_2C_2O_4$elution	Top-to-bottom	2.67
–	–	–	H_2SO_4 elution	Bottom-to-top	0.80	H_2SO_4 elution	Bottom-to-top	0.80
H_2O wash	Top-to-bottom	2.00	H_2O wash	Top-to-bottom	2.00	H_2O wash	Top-to-bottom	2.00

Flowrate 2.0 BV/h, except H_2O washes, at 6.0 BV/h, T = 60 °C.

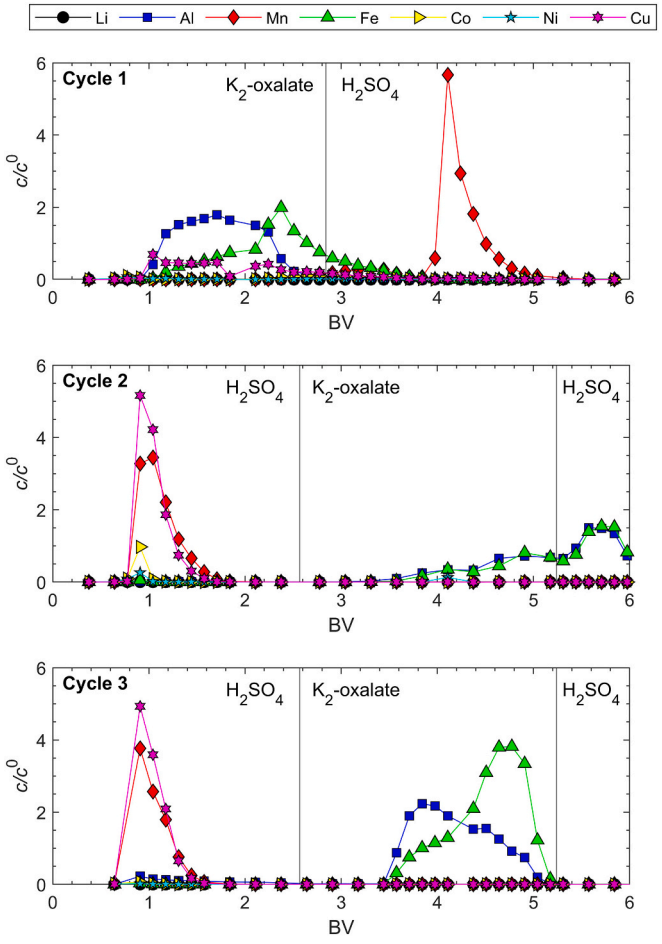

Fig. 8. Elution curves of three consecutive loading-elution ion exchange cycles for the removal of impurities from LIBWL with aminomethylphosphonic acid functional resin (Lewatit TP260). The flowrate in all steps was 2.0 BV/h, T = 60 °C. Other run parameters are presented in Table 6. The water wash steps are not presented in the figure.

the precipitation) due to the addition of chemicals for pH adjustment in every cycle.

The purpose of the H_2SO_4 regeneration step after the elutions is to convert the aminomethylphosphonic acid functional group of the resin from K^+ form to H^+ form. No metals enter into the 0.8 BV of the raffinate, which is acidic K_2SO_4 and also contains some oxalate from the empty volume of the bed. After the regeneration, the H_2SO_4 in the void volume of the resin bed is washed away with water before the loading step of the next cycle. The outcoming solution can be circulated to the H_2SO_4 feed tank.

Calculations based on the single-column ion exchange scheme suggested in Fig. 9, the productivities of the resulting solutions are as follows: >99.6% pure raffinate of Li, Co, and Ni 0.39 BV/h, Cu and Mn rich by-product 0.16 BV/h, and Fe and Al by-product 0.38 BV/h. The productivities can be improved by further optimizing the amounts and flowrates and using multicolumn set-ups, such as a lead-lag configuration. It must be noted that, if the flows are circulated internally in the process, as is suggested in the above discussion, the solution

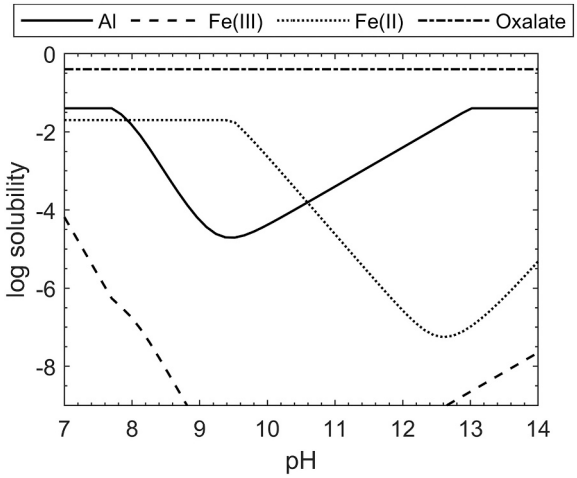

Fig. 10. Solubility curves for Al, Fe(II), Fe(III), and oxalate as a function of pH. Total concentrations are Al 0.04 mol/L, Fe 0.02 mol/L, oxalate 0.4 mol/L, and K 0.8 mol/L. T = 25 °C. The calculations have been performed with MEDUSA software (KTH Royal Institute of Technology, School of Chemical Engineering).

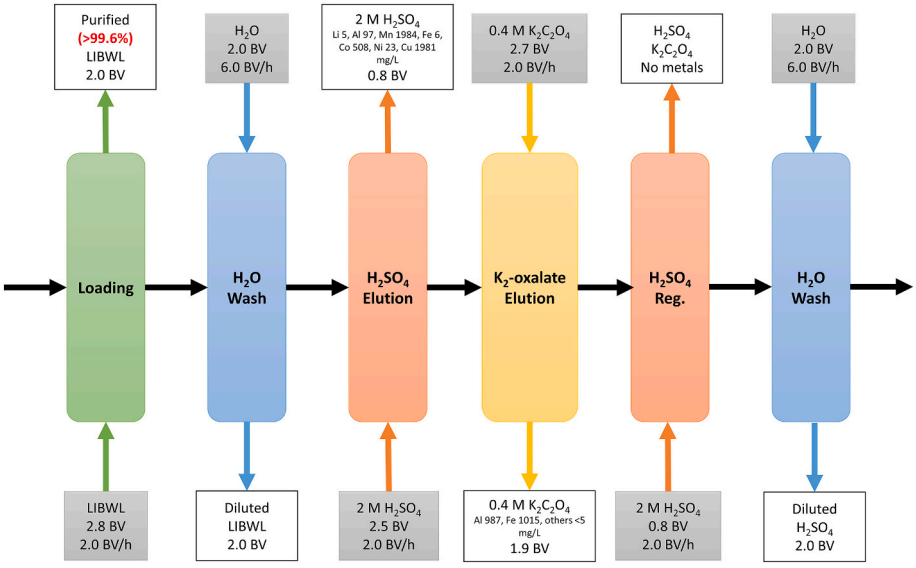

Fig. 9. Ion exchange process using aminomethylphosphonic acid functional Lewatit TP260 resin for the removal of impurities (Al, Fe, Mn, Cu) from LIBWL. Black arrows demonstrate the shift of the column from one step to another.

compositions in the feed tanks change dynamically. This must be considered in further process development with, for example, the addition of chemicals and/or evaporators to increase the concentrations.

4. Conclusions

The initial ion exchange process design was performed experimentally for the removal of impurities (Fe, Al, Mn, and Cu) from lithium ion battery waste leachate. All the experiments, except the batch elution experiments, were done in laboratory-scale columns. First, a suitable separation material was chosen. Normal strong and weak cation exchangers (Finex CS12GC and Finex CA16GC) could not remove the impurities selectively over the valuable Li, Co, and Ni; iminodiacetic acid chelating resin (Purolite S-930) could remove Fe and Cu, and aminomethylphosphonic acid chelating resin (Lewatit TP260) could remove all the desired metals. Increasing the temperature and pH of the feed solution were found to enhance separation performance. The optimal feed pH was 1.8 because, above this value, iron(III) precipitates as fine hydroxide, which is difficult to remove and cannot be fed to the column, due to clogging.

The elution of Fe and Al requires some chelator or a very high mineral acid concentration. Among citrate, oxalate, and EDTA, oxalate was evaluated as the best option. However, oxalate cannot remove Mn and causes Cu to precipitate in the column. This mandates a two-step elution approach, in which Cu and Mn are first eluted with 2 M H_2SO_4 and Fe and Al are eluted with 0.4 M oxalate. With this kind of design, 0.39 BV/h $>$ 99.6% pure battery grade Li, Co and Ni solution and 0.16 BV/h Cu and Mn rich H_2SO_4 solution and 0.38 BV/h Fe and Al oxalate solutions as by-products were produced. The productivities can be further optimized because, in this research only proof of concept was demonstrated. The cobalt losses were only 1.1% from the feed to the eluates, which is significantly less than those observed in conventional precipitation and solvent extraction purification processes. Also, in this case, the removal of all four impurity metals is accomplished in a single ion exchange process, while in the previously suggested approaches, several process steps are needed.

Declaration of Competing Interest

The authors declare that they have no known competing financial interests or personal relationships that could have appeared to influence the work reported in this paper.

Acknowledgements

The authors gratefully acknowledge financial support from 1) The Metal Producer's Fund (Finland) and 2) Business Finland (decision number 5715/31/2018) as part of the BATCircle (Finland-based Circular Ecosystem of Battery Metals) consortium.

References

Behal, I., Kumar, H., 2017. Exploring molecular interactions of aliphatic α-amino acids glycine, l-alanine, l-valine in aqueous potassium oxalate solutions from 288.15K to 318.15K through thermo-acoustical analysis. J. Mol. Liq. 244, 27–38. https://doi.org/10.1016/j.molliq.2017.08.103.

Chai, G., Cao, D., Zhang, M., Wang, J., Li, L., Chen, T., Li, W., Wang, Y., Wang, G., Guo, P., Wu, F., 2019a. Method for Recovering Valuable Metals in Waste Lithium Cobaltate Battery by Ion Exchange Method (CN 110468280 A 20191119).

Chai, G., Cao, D., Zhang, M., Wang, J., Li, L., Chen, T., Li, W., Wang, Y., Wang, G., Guo, P., 2019b. Method for Recovering Valuable Metal in Waste Nickel Cobalt Manganese Lithium Ion Battery by Ion Exchange Method (CN 110527836 A 20191203).

Chen, L., Tang, X., Zhang, Yang, Li, L., Zeng, Z., Zhang, Yi, 2011. Process for the recovery of cobalt oxalate from spent lithium-ion batteries. Hydrometallurgy 108, 80–86. https://doi.org/10.1016/j.hydromet.2011.02.010.

Chen, X., Chen, Y., Zhou, T., Liu, D., Hu, H., Fan, S., 2015a. Hydrometallurgical recovery of metal values from sulfuric acid leaching liquor of spent lithium-ion batteries. Waste Manag. 38, 349–356. https://doi.org/10.1016/j.wasman.2014.12.023.

Chen, X., Xu, B., Zhou, T., Liu, D., Hu, H., Fan, S., 2015b. Separation and recovery of metal values from leaching liquor of mixed-type of spent lithium-ion batteries. Sep. Purif. Technol. 144, 197–205. https://doi.org/10.1016/j.seppur.2015.02.006.

Cheng, C.Y., 2000. Purification of synthetic laterite leach solution by solvent extraction using D2EHPA. Hydrometallurgy 56, 369–386. https://doi.org/10.1016/S0304-386X(00)00095-5.

Chiu, K.-L., Chen, W.-S., 2017. Recovery and separation of valuable metals from cathode materials of spent lithium-ion batteries (LIBs) by ion exchange. Sci. Adv. Mater. 9, 2155–2160. https://doi.org/10.1166/sam.2017.3214.

Christodoulou, E., Panias, D., Paspaliaris, I., 2013. Calculated solubility of trivalent iron and aluminum in oxalic acid solutions at 25 °C. Can. Metall. Q. https://doi.org/10.1179/cmq.2001.40.4.421.

Dorella, G., Mansur, M.B., 2007. A study of the separation of cobalt from spent Li-ion battery residues. J. Power Sources 170, 210–215. https://doi.org/10.1016/j.jpowsour.2007.04.025.

Ekberg, C., Petranikova, M., 2015. Lithium batteries recycling. In: Chagnes, J., Światowska, A. (Eds.), Lithium Process Chemistry, Resources, Extraction, Batteries, and Recycling, 1st ed. Elsevier, Amsterdam, pp. 233–267. https://doi.org/10.1016/B978-0-12-801417-2.00007-4.

Ferg, E.E., Schuldt, F., Schmidt, J., 2019. The challenges of a Li-ion starter lighting and ignition battery: a review from cradle to grave. J. Power Sources 423, 380–403. https://doi.org/10.1016/j.jpowsour.2019.03.063.

Ferreira, D.A., Prados, L.M.Z., Majuste, D., Mansur, M.B., 2009. Hydrometallurgical separation of aluminium, cobalt, copper and lithium from spent Li-ion batteries. J. Power Sources 187, 238–246. https://doi.org/10.1016/j.jpowsour.2008.10.077.

Fisher, K.G., Treadgold, L.G., 2008. Design considerations for the cobalt recovery circuit for the KOL (KOV) copper/cobalt refinery, DRC. In: ALTA Nickel Cobalt 2008. ALTA Metallurgical Services, Melbourne, Australia.

Flett, D., 2004. Cobalt-nickel separation in hydrometallurgy: a review. Chem. Sustain. Dev. 81–91.

Georgi-Maschler, T., Friedrich, B., Weyhe, R., Heegn, H., Rutz, M., 2012. Development of a recycling process for Li-ion batteries. J. Power Sources 207, 173–182. https://doi.org/10.1016/j.jpowsour.2012.01.152.

Harper, G., Sommerville, R., Kendrick, E., Driscoll, L., Slater, P., Stolkin, R., Walton, A., Christensen, P., Heidrich, O., Lambert, S., Abbott, A., Ryder, K., Gaines, L., Anderson, P., 2019. Recycling lithium-ion batteries from electric vehicles. Nature 575, 75–86. https://doi.org/10.1038/s41586-019-1682-5.

Harris, B., White, Carl, 2018. Process for the Recovery of Cobalt, Lithium, and Other Metals From Spent Lithium-based Batteries and Other Feeds (WO 2018223193 A1 20181213).

Jurrius, Y., Sole, K.C., Hardwick, E., 2014. Removal of copper and zinc from a cobalt electrolyte by ion exchange at Kamoto Copper Company's Luilu plant. In: Proceedings of the 7th International Symposium on Hydrometallurgy 2014 (Hydro 2014). Presented at the Hydrometallurgy 2014 (Hydro 2014); MetSoc; SME, TMS, Victoria, British Columbia, Canada.

Kang, J., Senanayake, G., Sohn, J., Shin, S.M., 2010. Recovery of cobalt sulfate from spent lithium ion batteries by reductive leaching and solvent extraction with Cyanex 272. Hydrometallurgy 100, 168–171. https://doi.org/10.1016/j.hydromet.2009.10.010.

LANXESS, 2011. Product Information Lewatit-MonoPlus-TP-260.

Li, L., Zhang, X., Li, M., Chen, R., Wu, F., Amine, K., Lu, J., 2018. The recycling of spent Lithium-ion batteries: a review of current processes and technologies. Electrochem. Energ. Rev. 1, 461–482. https://doi.org/10.1007/s41918-018-0012-1.

Lv, R., Hu, Y., Jia, Z., Li, R., Zhang, X., Liu, J., Fan, C., Feng, J., Zhang, L., Wang, Z., 2019. Removal of Iron(III) and aluminum ions from phosphoric acid–nitric acid solutions by S957 chelation resin: kinetics, dynamic adsorption, and elution. Ind. Eng. Chem. Res. 58, 21641–21648. https://doi.org/10.1021/acs.iecr.9b04682.

Mendes, F.D., Martins, A.H., 2005. Recovery of nickel and cobalt from acid leach pulp by ion exchange using chelating resin. Miner. Eng. 18, 945–954. https://doi.org/10.1016/j.mineng.2004.12.009.

Meshram, P., Pandey, P.D., Mankhand, T.R., 2015. Hydrometallurgical processing of spent lithium ion batteries (LIBs) in the presence of a reducing agent with emphasis on kinetics of leaching. Chem. Eng. J. 281, 418–427. https://doi.org/10.1016/j.cej.2015.06.071.

Meshram, P., Mishra, A., Abhilash, Sahu, R., 2020. Environmental impact of spent lithium ion batteries and green recycling perspectives by organic acids – a review. Chemosphere 242, 125291. https://doi.org/10.1016/j.chemosphere.2019.125291.

Nayl, A.A., Hamed, M.M., Rizk, S.E., 2015. Selective extraction and separation of metal values from leach liquor of mixed spent Li-ion batteries. J. Taiwan Inst. Chem. Eng. 55, 119–125. https://doi.org/10.1016/j.jtice.2015.04.006.

Peng, C., Chang, C., Wang, Z., Wilson, B.P., Liu, F., Lundström, M., 2020. Recovery of high-purity MnO_2 from the acid leaching solution of spent Li-ion batteries. JOM 72, 790–799. https://doi.org/10.1007/s11837-019-03785-1.

Perry, R.H., Green, D.W., Maloney, J.O., 1997. Perry's Chemical Engineers' Handbook. McGraw-Hill.

Porvali, A., Aaltonen, M., Ojanen, S., Velazquez-Martinez, O., Eronen, E., Liu, F., Wilson, B.P., Serna-Guerrero, R., Lundström, M., 2019. Mechanical and hydrometallurgical processes in HCl media for the recycling of valuable metals from Li-ion battery waste. Resour. Conserv. Recycl. 2019, 257–266. https://doi.org/10.1016/j.resconrec.2018.11.023.

Quintero-Almanza, D., Gamiño-Arroyo, Z., Sánchez-Cadena, L.E., Gómez-Castro, F.I., Uribe-Ramírez, A.R., Aguilera-Alvarado, A.F., Ocampo Carmona, L.M., 2019. Recovery of cobalt from spent Lithium-ion Mobile phone batteries using liquid–liquid extraction. Batteries 5, 44. https://doi.org/10.3390/batteries5020044.

Sainio, T., Suppula, I., 2015. Method for Purification of a Cobalt Containing Solution by Continuous Ion Exchange. U.S. Patent No. 20150361524.

Sattar, R., Ilyas, S., Bhatti, H.N., Ghaffar, A., 2019. Resource recovery of critically-rare metals by hydrometallurgical recycling of spent lithium ion batteries. Sep. Purif. Technol. 209, 725–733. https://doi.org/10.1016/j.seppur.2018.09.019.

Siqueira, P., Silva, C.D., Silva, I.D., 2011. Nickel and cobalt adsorption in an ion exchange resin as an alternative for treating the leached liquer. Rem-Revista Escola De Minas 64, 319–326. https://doi.org/10.1590/S0370-44672011000300010.

Soare, L.C., Lemaître, J., Bowen, P., Hofmann, H., 2006. A thermodynamic model for the precipitation of nanostructured copper oxalates. J. Cryst. Growth 289, 278–285. https://doi.org/10.1016/j.jcrysgro.2005.11.085.

Sole, K.C., Mooiman, M., Hardwick, E., 2016. Present and future applications of ion exchange in hydrometallurgy: an overview. In: Proceedings of International Ion Exchange Conference IEx 2016. Presented at the International Ion Exchange Conference IEx 2016. Society of Chemical Industry, Cambridge, United Kingdom.

Swain, B., Jeong, J., Lee, J., Lee, G.-H., Sohn, J.-S., 2007. Hydrometallurgical process for recovery of cobalt from waste cathodic active material generated during manufacturing of lithium ion batteries. J. Power Sources 167, 536–544. https://doi.org/10.1016/j.jpowsour.2007.02.046.

Verma, A., Kore, R., Corbin, D.R., Shiflett, M.B., 2019. Metal recovery using oxalate chemistry: a technical review. Ind. Eng. Chem. Res. 58, 15381–15393. https://doi.org/10.1021/acs.iecr.9b02598.

Virolainen, S., Holopainen, O., Maliarik, M., Sainio, T., 2019. Ion exchange purification of a silver nitrate electrolyte. Miner. Eng. 132, 175–182. https://doi.org/10.1016/j.mineng.2018.12.020.

Wang, H., Friedrich, B., 2015. Development of a highly efficient hydrometallurgical recycling process for automotive Li–ion batteries. J. Sustain. Metall. 1, 168–178. https://doi.org/10.1007/s40831-015-0016-6.

Winslow, K.M., Laux, S.J., Townsend, T.G., 2018. A review on the growing concern and potential management strategies of waste lithium-ion batteries. Resour. Conserv. Recycl. 129, 263–277. https://doi.org/10.1016/j.resconrec.2017.11.001.

Xiao, J., Li, J., Xu, Z., 2020. Challenges to future development of spent Lithium ion batteries recovery from environmental and technological perspectives. Environ. Sci. Technol. 54, 9–25. https://doi.org/10.1021/acs.est.9b03725.

Younesi, R., Veith, G.M., Johansson, P., Edström, K., Vegge, T., 2015. Lithium salts for advanced lithium batteries: Li–metal, Li–O_2, and Li–S. Energy Environ. Sci. 8, 1905–1922. https://doi.org/10.1039/C5EE01215E.

Zainol, Z., Nicol, M.J., 2009. Comparative study of chelating ion exchange resins for the recovery of nickel and cobalt from laterite leach tailings. Hydrometallurgy 96, 283–287. https://doi.org/10.1016/j.hydromet.2008.11.005.

Zeng, X., Li, J., Singh, N., 2014. Recycling of spent lithium-ion battery: a critical review. Crit. Rev. Environ. Sci. Technol. 44, 1129–1165. https://doi.org/10.1080/10643389.2013.763578.

Zhang, Y., Liu, Q., Li, L., 2016. Removal of iron from synthetic copper leach solution using a hydroxy-oxime chelating resin. Hydrometallurgy 164, 154–158. https://doi.org/10.1016/j.hydromet.2016.06.004.